Quantitative Analysis of the Transcription Control-Mechanism

Changhui Mao[1,3], Christopher R. Brown[1,3], Elena Falkovskaia[1,3], Shawfeng Dong[2], Eva Hrabeta-Robinson[1], Lauren Wenger[1], and Hinrich Boeger[1,*]

[1] Department of Molecular, Cell, and Developmental Biology, [2] Department of Astronomy and Astrophysics, University of California Santa Cruz, Santa Cruz, CA 95064, USA

Supplementary Information

Table of Contents

1. Mathematical Treatment of Expression Model

We define the space of *cellular PHO5 expression states* by

$$\Omega \equiv \{\mathbf{x} = (i,m,n) \,|\, i \in \{0,...,9\}, m \in \mathbb{N}_0, n \in \mathbb{N}_0\},$$

where *i* refers to promoter state E_i, *m* to the number of *PHO5* mRNA molecules, and *n* to the number of Pho5 protein molecules within a cell. We assumed that the probability for a transition from one cellular expression state into another only depends on the present and future state but not the cell's history ('memory-free' or time-homogeneous Markov process). This notion implies that dwell times between transitions are exponentially distributed (Feller, 1968). Thus, the probability of finding the cell in state $\mathbf{x}' \in \Omega$ at time $t + h$, given the cell was in state $\mathbf{x} \in \Omega$ at time *t*, equals

$$[1] \qquad P(\mathbf{x}', t+h \,|\, \mathbf{x}, t) = 1 - \exp[-\xi_{\mathbf{x}',\mathbf{x}} h],$$

where $\xi_{\mathbf{x}',\mathbf{x}}$ is a constant ≥ 0 (the transition probability per time), which only depends on the present state **x** and future state **x'**. Equation [1] implies

$$[2] \qquad \lim_{h \to 0} \frac{P(\mathbf{x}', t+h \,|\, \mathbf{x}, t)}{h} = \xi_{\mathbf{x}',\mathbf{x}}.$$

We assumed that the probability per time

for transitions between promoter states $(i,m,n) \to (j,m,n)$ is $\gamma_{j,i}$,

for promoter clearance transitions $(i,m,n) \to (i,m+1,n)$ is ε_i,

for transitions due to mRNA degradation $(i,m,n) \to (i,m-1,n)$ is $m\delta$,

for transitions due to translation $(i,m,n) \to (i,m,n+1)$ is $m\eta$,

for transitions due to protein degradation $(i,m,n) \to (i,m,n-1)$ is $n\zeta$,

where $\gamma_{j,i}$, ε_i, δ, η, and ζ are constants and $i, j \in \{0,...,9\}$. For simplicity, we refer to these constants (transition probabilities per time per molecule) as *kinetic parameters*. From these assumptions and [2] follows the chemical master equation of the stochastic expression process, which describes the flow of probability mass (Boeger et al., 2008):

$$[3] \qquad \frac{d}{dt} P_{i,m,n}(t) = \sum_{j \in \{0,...,9\}} \gamma_{i,j} P_{j,m,n}(t) - [m(\delta+\eta) + \zeta n + \varepsilon_i] P_{i,m,n}(t) + \delta(m+1) P_{i,m+1,n}(t) + \zeta(n+1) P_{i,m,n+1}(t) + \eta m P_{i,m,n-1}(t) + \varepsilon_i P_{i,m-1,n}(t),$$

where $P_{i,m,n}(t)$ is the probability of finding a cell in state (*i*,*m*,*n*) at time *t*, with

[4] $P_{i,m,n}(t) \equiv 0$ if $m < 0$, or $n < 0$, and

[5] $\gamma_{i,i} \equiv - \sum_{j \in \{0,...,9\} \setminus \{i\}} \gamma_{i,j}$ for all $i \in \{0,...,9\}$.

Equation [5] is a consequence of probability mass conservation, which requires that the probability mass flowing out of promoter state E_i equals the mass that other promoters states E_j receive from E_i. Analytical solutions for the first and second moments of the steady-state (stationary state) joint probability distribution for which $\frac{d}{dt} P_{i,m,n}(t) = 0$ for all i, m, and n, were derived from [3] using vector-valued generating functions (Boeger et al., 2008). Here, we reproduce this derivation, filling in steps that previously had been omitted for the sake of brevity.

Let

[6] $$\mathbf{P}(m,n,t) \equiv (P_{0,m,n}(t),...,P_{9,m,n}(t))^T,$$
$$\Gamma \equiv (\gamma_{i,j}),$$
$$E \equiv (\varepsilon_i \delta_{i,j}),$$

where Γ and E are 10 x 10 matrices, $\delta_{i,j}$ is the Kronecker symbol, that is $\delta_{i,j} \equiv 1$ if $i = j$ but 0 otherwise, and the superscript T indicates that $\mathbf{P}(m,n,t)$ is to be understood as a column vector, although it is written in row-form. With definitions [6], the master equation [3] can be rewritten in vector form

[7] $$\frac{d}{dt}\mathbf{P}(m,n,t) = \Gamma\mathbf{P}(m,n,t) - m(\delta+\eta)\mathbf{P}(m,n,t) - \zeta n\mathbf{P}(m,n,t) + \delta(m+1)\mathbf{P}(m+1,n,t)$$
$$+ \zeta(n+1)\mathbf{P}(m,n+1,t) + \eta m\mathbf{P}(m,n-1,t) + E\mathbf{P}(m-1,n,t) - E\mathbf{P}(m,n,t).$$

We define the vector-valued generating function

[8] $\mathbf{G}(y,z,t) \equiv \sum_{m,n \geq 0} y^m z^n \mathbf{P}(m,n,t)$ for all $t \in \mathbb{R}_{\geq 0}$, and all $y,z \in [0,1]$,

which will allow us to calculate variance and mean for the number of protein molecules at steady-state (equation [15]). Obviously, $\mathbf{G}(1,1,t) \equiv \mathbf{p}(t) = (p_0(t),...,p_9(t))^T$, where p_i, the ith component function of $\mathbf{p}$, indicates the probability of finding the promoter in state i at time t. Partial differentiation of [8] yields

$$\frac{\partial}{\partial y}\mathbf{G}(y,z,t)=\sum_{\substack{m\geq 1\\ n\geq 0}} m y^{m-1}z^{n}\mathbf{P}(m,n,t)=\sum_{m,n\geq 0}(m+1)y^{m}z^{n}\mathbf{P}(m+1,n,t)$$

$$y\frac{\partial}{\partial y}\mathbf{G}(y,z,t)=y\sum_{\substack{m\geq 1\\ n\geq 0}} m y^{m-1}z^{n}\mathbf{P}(m,n,t)=\sum_{m,n\geq 0} m y^{m}z^{n}\mathbf{P}(m,n,t)$$

$$\frac{\partial}{\partial z}\mathbf{G}(y,z,t)=\sum_{\substack{n\geq 1\\ m\geq 0}} n y^{m}z^{n-1}\mathbf{P}(m,n,t)=\sum_{m,n\geq 0}(n+1)y^{m}z^{n}\mathbf{P}(m,n+1,t)$$

[9]

$$z\frac{\partial}{\partial z}\mathbf{G}(y,z,t)=z\sum_{\substack{n\in\geq 1\\ m\geq 0}} n y^{m}z^{n-1}\mathbf{P}(m,n,t)=\sum_{m,n\geq 0} n y^{m}z^{n}\mathbf{P}(m,n,t)$$

$$yz\frac{\partial}{\partial y}\mathbf{G}(y,z,t)=\sum_{\substack{m\geq 1\\ n\geq 0}} m y^{m}z^{n+1}\mathbf{P}(m,n,t)=\sum_{m,n\geq 1} m y^{m}z^{n}\mathbf{P}(m,n-1,t)$$

$$=\sum_{m,n\geq 0} m y^{m}z^{n}\mathbf{P}(m,n-1,t)\ ,$$

where the last equality sign makes use of definition [4]. From [8] follows

[10] $$\frac{\partial}{\partial t}\mathbf{G}(y,z,t)\equiv\sum_{m,n\in\mathbf{N}_0} y^{m}z^{n}\frac{d}{dt}\mathbf{P}(m,n,t)\ .$$

Inserting [7] into [10], and using equations [9] gives

[11]
$$\frac{\partial}{\partial t}\mathbf{G}(y,z,t)=\Gamma\mathbf{G}(y,z,t)+\delta(1-y)\frac{\partial}{\partial y}\mathbf{G}(y,z,t)+\zeta(1-z)\frac{\partial}{\partial z}\mathbf{G}(y,z,t)$$
$$-\eta(1-z)y\frac{\partial}{\partial y}\mathbf{G}(y,z,t)-(1-y)E\mathbf{G}(y,z,t).$$

By partial differentiation of [11], we obtain

[12]
$$\frac{\partial^2}{\partial y\partial t}\mathbf{G}(y,z,t)=\Gamma\frac{\partial}{\partial y}\mathbf{G}(y,z,t)+\delta(1-y)\frac{\partial^2}{\partial y^2}\mathbf{G}(y,z,t)-\delta\frac{\partial}{\partial y}\mathbf{G}(y,z,t)$$
$$+\zeta(1-z)\frac{\partial^2}{\partial y\partial z}\mathbf{G}(y,z,t)-\eta(1-z)\frac{\partial}{\partial y}\mathbf{G}(y,z,t)-\eta(1-z)y\frac{\partial^2}{\partial y^2}\mathbf{G}(y,z,t)$$
$$-(1-y)\mathrm{E}\frac{\partial}{\partial y}\mathbf{G}(y,z,t)+E\mathbf{G}(y,z,t)\ ,$$

[13]
$$\frac{\partial^2}{\partial z\partial t}\mathbf{G}(y,z,t)=\Gamma\frac{\partial}{\partial z}\mathbf{G}(y,z,t)+\delta(1-y)\frac{\partial^2}{\partial z\partial y}\mathbf{G}(y,z,t)+\zeta(1-z)\frac{\partial^2}{\partial z^2}\mathbf{G}(y,z,t)$$
$$-\zeta\frac{\partial}{\partial z}\mathbf{G}(y,z,t)-\eta(1-z)y\frac{\partial^2}{\partial z\partial y}\mathbf{G}(y,z,t)+\eta y\frac{\partial}{\partial y}\mathbf{G}(y,z,t)$$
$$-(1-y)E\frac{\partial}{\partial z}\mathbf{G}(y,z,t)\ .$$

Further differentiation of [12] and [13] gives

$$\frac{\partial^3}{\partial y^2\partial t}\mathbf{G}(y,z,t)=\Gamma\frac{\partial^2}{\partial y^2}\mathbf{G}(y,z,t)+\delta(1-y)\frac{\partial^3}{\partial y^3}\mathbf{G}(y,z,t)-2\delta\frac{\partial^2}{\partial y^2}\mathbf{G}(y,z,t)$$
$$+\zeta(1-z)\frac{\partial^3}{\partial y^2\partial z}\mathbf{G}(y,z,t)-\eta(1-z)\frac{\partial^2}{\partial y^2}\mathbf{G}(y,z,t)-\eta(1-z)y\frac{\partial^3}{\partial y^3}\mathbf{G}(y,z,t) \quad [14]$$
$$-\eta(1-z)\frac{\partial^2}{\partial y^2}\mathbf{G}(y,z,t)-(1-y)E\frac{\partial^2}{\partial y^2}\mathbf{G}(y,z,t)+2E\frac{\partial}{\partial y}\mathbf{G}(y,z,t)\ ,$$

$$\frac{\partial^3}{\partial z^2\partial t}\mathbf{G}(y,z,t)=\Gamma\frac{\partial^2}{\partial z^2}\mathbf{G}(y,z,t)+\delta(1-y)\frac{\partial^3}{\partial z^2\partial y}\mathbf{G}(y,z,t)+\zeta(1-z)\frac{\partial^3}{\partial z^3}\mathbf{G}(y,z,t)$$
$$-2\zeta\frac{\partial^2}{\partial z^2}\mathbf{G}(y,z,t)-\eta(1-z)y\frac{\partial^3}{\partial z^2\partial y}\mathbf{G}(y,z,t)+2\eta y\frac{\partial^2}{\partial z\partial y}\mathbf{G}(y,z,t) \quad [15]$$
$$-(1-y)E\frac{\partial^2}{\partial z^2}\mathbf{G}(y,z,t)\ ,$$

$$\frac{\partial^3}{\partial z\partial y\partial t}\mathbf{G}(y,z,t)=\Gamma\frac{\partial^2}{\partial z\partial y}\mathbf{G}(y,z,t)+\delta(1-y)\frac{\partial^3}{\partial z\partial y^2}\mathbf{G}(y,z,t)-\delta\frac{\partial^2}{\partial z\partial y}\mathbf{G}(y,z,t)$$
$$+\zeta(1-z)\frac{\partial^3}{\partial y\partial z^2}\mathbf{G}(y,z,t)-\zeta\frac{\partial^2}{\partial y\partial z}\mathbf{G}(y,z,t)-\eta(1-z)\frac{\partial^2}{\partial z\partial y}\mathbf{G}(y,z,t)$$
$$+\eta\frac{\partial}{\partial y}\mathbf{G}(y,z,t)-\eta(1-z)y\frac{\partial^3}{\partial z\partial y^2}\mathbf{G}(y,z,t)+\eta y\frac{\partial^2}{\partial y^2}\mathbf{G}(y,z,t) \quad [16]$$
$$-(1-y)E\frac{\partial^2}{\partial z\partial y}\mathbf{G}(y,z,t)+E\frac{\partial}{\partial z}\mathbf{G}(y,z,t).$$

We now define the generating function

$$G(y,z,t)\equiv\sum_{i=0}^{9}G_i(y,z,t)\equiv\left\|\mathbf{G}(y,z,t)\right\|\ , \quad [17]$$

where G_i is the i[th] component function of **G**. The mean values and variances of mRNA and protein molecules can be derived from G according to

$$\mu_M(t)=\frac{\partial}{\partial y}G(1,1,t)\ ,\ \mu_N(t)=\frac{\partial}{\partial z}G(1,1,t),\ Cov_{M,N}(t)=\frac{\partial^2}{\partial y\partial z}G(1,1,t)-\mu_M(t)\mu_N(t)$$
$$\sigma_M^2(t)=\frac{\partial^2}{\partial y^2}G(1,1,t)+\mu_M(t)-\mu_M^2(t)\ ,\ \sigma_N^2(t)=\frac{\partial^2}{\partial z^2}G(1,1,t)+\mu_N(t)-\mu_N^2(t)\ , \quad [18]$$

where $\mu_M(t)$ is the mean value of mRNA molecules, $\mu_N(t)$ is the mean number of protein molecules, $Cov_{M,N}(t)$ is the covariance of mRNA and protein expression, $\sigma_M^2(t)$ is the variance of mRNA

molecules, and $\sigma_N^2(t)$ is the variance of protein molecules at time *t*. The first three equations follow directly from the definitions. The forth equation follows from

$$\begin{aligned}\frac{\partial^2}{\partial y^2}G(1,1,t) &= \sum_{m\geq 2}\sum_{n\geq 0} m(m-1)\|\mathbf{P}(m,n,t)\| \\ &= \sum_{m\geq 2}\sum_{n\geq 0} m^2\|\mathbf{P}(m,n,t)\| - \sum_{m\geq 2}\sum_{n\geq 0} m\|\mathbf{P}(m,n,t)\| \\ &= \sum_{m,n\geq 0} m^2\|\mathbf{P}(m,n,t)\| - \sum_{m,n\geq 0} m\|\mathbf{P}(m,n,t)\|\end{aligned}$$

and $\sigma_M^2(t) = \sum_{n,m\geq 0} m^2\|\mathbf{P}(m,n,t)\| - [\mu_M(t)]^2$. An equivalent argument applies for the last equation.

If there is a stationary joint distribution $\bar{P}(i,m,n)$, it is uniquely determined and

[19] $\lim_{t\to\infty} P_{i,m,n}(t) = \bar{P}(i,m,n)$ for all *i*, *m*, *n* (Grimmett and Stirzaker, 2001).

Thus, $\lim_{t\to\infty}\frac{\partial}{\partial y}\mathbf{G}(1,1,t) \equiv \mathbf{v}$, $\lim_{t\to\infty}\frac{\partial}{\partial z}\mathbf{G}(1,1,t) \equiv \mathbf{w}$, and $\lim_{t\to\infty}\mathbf{G}(1,1,t) \equiv \mathbf{p}$ exist. By taking the limit for $t\to\infty$, we obtain from [11] - [13] the following set of linear equations

[20]
$$\begin{aligned}\Gamma\mathbf{p} &= \mathbf{0} \\ (\delta\, Id - \Gamma)\mathbf{v} &= E\mathbf{p} \\ (\zeta\, Id - \Gamma)\mathbf{w} &= \eta\mathbf{v}\ ,\end{aligned}$$

where Id is the identity matrix $(\delta_{i,j})$. With [18] follows

[21] $\|\mathbf{v}\| = \mu_M$, and $\|\mathbf{w}\| = \mu_N$,

with μ_M and μ_N the stationary mean values for mRNA and protein, respectively.

Because of [19], $\mathbf{r} \equiv \lim_{t\to\infty}\frac{\partial^2}{\partial y^2}\mathbf{G}(1,1,t)$, $\mathbf{s} \equiv \lim_{t\to\infty}\frac{\partial^2}{\partial z^2}\mathbf{G}(1,1,t)$, and $\mathbf{u} \equiv \lim_{t\to\infty}\frac{\partial^2}{\partial y\partial z}\mathbf{G}(1,1,t)$ exist, and from equations [14] – [16] follows, taking the limit for $t\to\infty$,

[22]
$$\begin{aligned}(2\delta\, Id - \Gamma)\mathbf{r} &= 2E\mathbf{v} \\ (2\zeta\, Id - \Gamma)\mathbf{s} &= 2\eta\mathbf{u} \\ [(\delta+\zeta)Id - \Gamma]\mathbf{u} &= \eta\mathbf{v} + \eta\mathbf{r} + E\mathbf{w}\end{aligned}$$

The last two equations of [22] can be combined to eliminate **u**, which gives

$$[(\delta+\zeta)Id - \Gamma][2\zeta\, Id - \Gamma]\mathbf{s} = 2\eta E\mathbf{w} + 2\eta^2\mathbf{v} + 2\eta^2\mathbf{r}.$$

According to [18],

$$Cov_{M,N} = \|\mathbf{u}\| - \|\mathbf{v}\|\|\mathbf{w}\|$$

[23] $$\sigma_M^2 = \|\mathbf{r}\| + \|\mathbf{v}\| - \|\mathbf{v}\|^2$$

$$\sigma_N^2 = \|\mathbf{s}\| + \|\mathbf{w}\| - \|\mathbf{w}\|^2 ,$$

where $Cov_{M,N}$, σ_M^2, and σ_N^2 are the covariance, and the variances of mRNA and protein expression at steady state, respectively. Thus, the stationary probabilities of nucleosome configurations E_i, and the stationary mean values, variances, and the covariance of the gene products can be deduced by solving the system of vector equations

$$\Gamma\mathbf{p} = \mathbf{0}$$

$$(\delta\ Id - \Gamma)\mathbf{v} = E\mathbf{p}$$

$$(\zeta\ Id - \Gamma)\mathbf{w} = \eta\mathbf{v}$$

[24] $$(2\delta\ Id - \Gamma)\mathbf{r} = 2E\mathbf{v}$$

$$[(\delta + \zeta)Id - \Gamma][2\zeta\ Id - \Gamma]\mathbf{s} = 2\eta E\mathbf{w} + 2\eta^2\mathbf{v} + 2\eta^2\mathbf{r}$$

$$[(\delta + \zeta)Id - \Gamma]\mathbf{u} = \eta\mathbf{v} + \eta\mathbf{r} + E\mathbf{w}\ .$$

Equation [5] implies $\det\Gamma = 0$. Hence, the first equation of [24] has a nontrivial solution. Using mathematical software packages capable of symbolic calculations, for example Mathematica (Wolfram Research), it can be seen that the rank of the 10 x 10 matrix Γ equals 9 for the transition topology of Fig. 5, which implies that the kernel of Γ has dimension 1. Hence, $\Gamma\mathbf{p} = \mathbf{0}$ uniquely defines **p**, given that $\|\mathbf{p}\| = 1$, per definition. Model predictions for the experimental observables were calculated using [21], and

[25] $$\mu_X = X\mathbf{p}\ \text{, where } X \equiv (0,1,1,1,2,2,2,1,2,2)\ ,$$

[26] $$\eta_{\text{int}}^2 \equiv \frac{\sigma_N^2}{\mu_N^2}\ .$$

The i[th] component of vector X refers to the number of nucleosomes lost in promoter state E_i (Fig. 5A). We note that model calculations treat the kinetic parameters as constants. Calculated noise, therefore, is intrinsic noise, and not total or extrinsic noise.

2. Formal Characterization of Regulatory Schemes

We allowed for eight independent kinetic parameters $z_1,...,z_8$, where z_1 describes transitions from 2-nucleosome to the 3-nucleosome states (thus $\gamma_{0,j} \equiv z_1$ for j = 1, 2, 3), z_2 refers to transitions from 1-nucleosome to the 2-nucleosome states, z_3 refers to sliding transitions, z_4 pertains

to nucleosome disassembly transitions. Parameter z_5 and z_6 describe transitions into and out of transcriptionally active states, respectively, and parameters z_7 and z_8 refer to promoter clearance and translation, respectively. Thus, $\varepsilon_7, \varepsilon_8, \varepsilon_9 = z_7$, whereas all other $\varepsilon_j \equiv 0$ in accordance with Premise 3, and $z_8 = \eta$. The set of all parameter vectors $(z_1,...,z_8)$ constitutes the *parameter space* $P \subseteq \mathbb{R}^8_{\geq 0}$. For any kinetic parameter vector $(z_1,...,z_8)$ the Markov chain model F, specified by the chemical master equation [3], allows for the calculation of the experimental observables μ_X, μ_N, and η^2_{int} (see equations [21], [25], and [26]). Thus,

$$F : P \subseteq \mathbb{R}^8_{\geq 0} \to D \subseteq \mathbb{R}^3_{\geq 0} \text{ with } (z_1,...,z_8) \mapsto (\mu_X, \mu_N, \eta^2_{\text{int}}).$$

The set $D \subseteq \mathbb{R}^3_{\geq 0}$ of all vectors $(\mu_X, \mu_N, \eta^2_{\text{int}})$ is called the *data space*, and we refer to its elements as *macroscopic expression states*. The kinetic parameter vector thus fully determines the macroscopic expression state.

Let $\boldsymbol{\omega} = (\omega_1,...,\omega_8) \in P$ be the parameter vector for the *PHO4 pho80*Δ strain. A mutation in the Pho4p activation domain alters the kinetic parameters that pertain to the activator-controlled transitions of *PHO5* expression. A scheme $S_{i,j}$ that assumes activator regulation of two parameters can be represented by the mapping

[27] $$\Lambda(\boldsymbol{\omega}, S_{i,j}) : A \subset \mathbb{R}^2_{>0} \to P \text{, with} \in (x,y) \mapsto (\omega_1,...,x\omega_i,...,y\omega_j,...,\omega_8),$$

where A, the *coordinate space*, is the rectangle $(0,L]^2$ for some number $L > 1$. Every *pho4* mutant is represented by a pair of numbers $(x,y) \in A$. By definition, the pair $(1,1) \in A$ represents the *PHO4* wild type. With the assignments for parameters z_j as given above, $S_{4,5}$ represent regulatory schemes I, $S_{4,7}$ is scheme II, and $S_{5,7}$ is scheme III.

With $\mathbf{a} = (\omega_1,...,0_i,...,0_j,...,\omega_8)$, $\mathbf{b} = (0,...,1_i,...,0)$, and $\mathbf{c} = (0,...,1_j,...,0) \in P$,

$(\omega_1,...,x\omega_i,...,y\omega_j,...,\omega_8) = \mathbf{a} + x\mathbf{b} + y\mathbf{c}$.

The latter equation shows that the image of A under $\Lambda(\boldsymbol{\omega}, S_{i,j})$, is a 2-dimensional tangent plane to **a** in P spanned by vectors **b** and **c**. The image of A under the composite mapping

[28] $$F \circ \Lambda(\boldsymbol{\omega}, S_{i,j}) : A \subset \mathbb{R}^2_{>0} \to D \subseteq \mathbb{R}^3_{\geq 0} \text{, with } (x,y) \mapsto (\mu_X, \mu_N, \eta^2_{\text{int}})$$

is a surface in $D \subseteq \mathbb{R}^3_{\geq 0}$ (2-dimensional manifold with boundary). Hence, a two-step regulatory process predicts that all macroscopic expression states generated by mutations in the Pho4p activation

domain are confined to a surface in data space. Different regulatory schemes $S_{i,j}$ are represented by different tangent planes in *P*, and different surfaces in *D*. Thus, answering the question of which steps of the gene expression process are activator-controlled, requires identification of the tangent plane in *P* whose image under *F* fits the experimental data in *D* best. How this task was addressed is described in the next paragraph.

3. Parameter Fitting

Given the two-step regulatory scheme $S_{i,j}$ and wild type parameter vector $\boldsymbol{\omega}$, the observables μ_X, μ_N and η^2_{int} become functions of the coordinates x and y (see [28]). Thus $\mu_X = \mu_X(x,y)$, $\mu_N = \mu_N(x,y)$, $\eta^2_{\text{int}} = \eta^2_{\text{int}}(x,y)$.

Experimentally, we expressed the level of expression relative to wild type expression. To align theoretical values with measured values, we calculated $\mu_N(x,y)/\mu_N(1,1)$ (see comments to [27]). In the following, we will refer to this ratio simply as $\mu_N(x,y)$.

Let $\mu_X^{(n)}$, $\mu_N^{(n)}$ and $(\eta^2_{\text{int}})^{(n)}$ be the observables for mutant *n*. Using the Newton-Raphson method, we solved the system of equations

[29]
$$\begin{aligned}\mu_X(x,y) &= \mu_X^{(n)}\\ \mu_N(x,y) &= \mu_N^{(n)}\end{aligned}$$

for *x* and *y* to obtain

[30]
$$\begin{aligned}x^{(n)} &= x(\mu_X^{(n)},\mu_N^{(n)})\\ y^{(n)} &= y(\mu_X^{(n)},\mu_N^{(n)})\end{aligned}$$

for all *n*. This was done by iteratively solving

$$(\mu_X^{(n)},\mu_N^{(n)})^T - \Psi(x_j,y_j) = J_\Psi(x_j,y_j)(x_{j+1}-x_j, y_{j+1}-y_j)^T$$

for x_{j+1} and y_{j+1} until convergence, where $\Psi(x_j,y_j) \equiv (\mu_X(x,y),\mu_N(x,y))^T$, and $J_\Psi(x,y)$ is the Jacobian matrix of Ψ at (x,y), thus

$$J_\Psi(x,y) = \begin{pmatrix} \frac{\partial}{\partial x}\mu_X(x,y) & \frac{\partial}{\partial y}\mu_X(x,y) \\ \frac{\partial}{\partial x}\mu_N(x,y) & \frac{\partial}{\partial y}\mu_N(x,y) \end{pmatrix}.$$

Iterations were initiated at $(x_0, y_0) \equiv (1,1)$. Solutions [30] were used to calculate the expected (theoretical) intrinsic noise of expression

[31] $$\eta^2_{\text{int}}(x^{(n)}, y^{(n)}) = \eta^2_{\text{int}}(\mu_X^{(n)}, \mu_N^{(n)}),$$

for activator mutants $n = 1,\ldots, N$.

To determine the error between expected noise $\eta^2_{\text{int}}(\mu_X^{(n)}, \mu_N^{(n)})$ and measured noise $(\eta^2_{\text{int}})^{(n)}$, we define the error function $\Delta(\boldsymbol{\omega}, S_{i,j}) : P \mapsto \mathbb{R}_{\geq 0}$, with

[32] $$\Delta(\boldsymbol{\omega}, S_{i,j}) \equiv \frac{1}{N}\sum_{n=1}^{N}\left|\log_{10}[\eta^2_{\text{int}}(\mu_X^{(n)}, \mu_N^{(n)})] - \log_{10}[(\eta^2_{\text{int}})^{(n)}]\right| .$$

Thus, if $\Delta(\boldsymbol{\omega}, S_{i,j}) = 0$, the model accounts for the experimentally observed quantitative relationships between μ_X, μ_N and η^2_{int} with perfect accuracy. We note that our approach assured that calculated and measured values for μ_X and μ_N agreed for all mutants, all regulatory schemes, and all $\boldsymbol{\omega}$ (see equations [29] and [30]).

The error function $\Delta(\boldsymbol{\omega}, S_{i,j})$ was minimized on the parameter space P using the Nelder-Mead simplex algorithm (Nelder and Mead, 1965), with standard values $\alpha = 1$, $\gamma = 2$, $\rho = 0.5$, and $\sigma = 0.5$ for the reflection, expansion, contraction and shrink coefficient, respectively. To search for a global minimum of $\Delta(\boldsymbol{\omega}, S_{i,j})$ on P, we took a Monte Carlo approach: We used a random number generator to determine the *central vertex* of the starting simplex for the Nelder-Mead algorithm; each of the remaining eight vertices was then calculated by adding 50 h^{-1} to one of the eight component values of the central vertex. The *best-fit solution*, given scheme $S_{i,j}$, is defined as the parameter vector that gave the smallest error for 16,000 different starting simplexes.

4. Model Testing

To test regulatory scheme I, we recalculated the model parameters using the data for 17 rather than 21 strains. The calculated parameters were similar to the previously calculated parameters and well predicted the intrinsic noise values of mutants that were not included in the fitting (Table S2, and Fig. S6).

5. Calculations

Calculations for different starting simplexes were performed in parallel, and run on an 8-core Mac Pro computer using Grand Central Dispatch (GCD) for multicore computing (introduced with Mac OS X version 10.6 Snow Leopard). Parallelization with GCD allowed us to calculate model parameters for individual regulatory schemes in less than three hours. Programs for parameter fitting were written in C. The surface representation of intrinsic noise as a function of expression level and nucleosome loss in Figure 7 was calculated using Mathematica 7 (Wolfram Research).

6. Flow Cytometry

PHO5 promoter-controlled expression was evaluated in haploid strains by FACS analysis using a FACSAria instrument (BD Biosciences) equipped with a 70 μm nozzle and controlled by the DIVA acquisition program (BD Biosciences). The level of expression for each *PHO4* mutant strain was referenced to strain yE1.1 (*PHO4 pho80Δ)*, which was measured in parallel. The level of yE1.1 expression was set to 1. Strain yE3.1 (*pho4Δ pho80Δ*) was employed as a negative control to measure the level of autofluorescence. The YFP fluorescence was collected in the FITC channel (laser excitation at 488 nm; HQ530/30 nm band-pass filter).

For the expression analysis cells were grown in SCD medium. Prior to FACS measurements cells were filtered through a 70 μm nylon mesh and briefly sonicated. Data from 50,000 cells were collected for each measurement using the "Area" option; each sample was re-measured at least four times. No less than two independent cell cultures at two different cell density levels were evaluated for each *PHO4* mutant strain.

Data from flow cytometry measurements were exported from DIVA as FSC3.0 files and data analysis was carried out by FlowJo software (Tree Star, Inc.). Data processing was performed according to the following rules to insure the quality of the cell population: First, dead cells were excluded based on staining with propidium iodide (PI) (~ 1%). Second, to limit contributions from cell debris and cell aggregates, cells were selected for size in the FSC channel (forward scattering) to include cells between 25,000 – 150,000 arbitrary units. In the SSC channel (side scattering) the top and bottom 2% of the cells were excluded. This procedure reduced the number of cells by 20-25%. Third, obvious outliers were identified visually in YFP versus PI color density plots. This additional step eliminated less than 1% of the remaining cells.

7. Fluorescent In Situ Hybridization

The DNA oligonucleotides were designed to probe the CFP mRNA using the *Designer* function of the www.singlemoleculefish.com site (Raj et al., 2006). Five 50 nucleotide-long probes spanning the 5'-end of the open reading frame that had a GC content of at least 40% were chosen for this study. The oligonucleotide sequences were:

GACCARTAACATCACCARCTAATTCAACCAAAARTGGGACAACACCAGRG ,

GGRCAATTTACCGRAAGTAGCARCACCTTCACCTRCACCGGAGACAGAAA ,

CCCCAAGRTAAAGTAGTGACRAAGGTTGGCCARGGAACTGGCAATTRACC ,

CCTTCRGGCATGGCAGACTRGAAAAAGTCATGRTGTTTCATATGATCRGGG ,

CACCRTCAAACTRGACTTCAGCTCTGGTCTRGTAGTTACCGTCARCTTTG ,

where R indicates incorporation of amino-modified deoxythymidine (four modified sites per probe). Probes were purchased from BioSearch Technologies, Inc. The free amines were coupled to Alexa555 fluorophore (Invitrogen, A20009) according to the manufacture's specification with the following modifications: 200 mM sodium bicarbonate, pH8.5 buffer containing 10% (v/v) of DMSO was used for overnight room temperature reaction. Labeling reaction was ethanol precipitated once to remove the free dye molecules and further purified by HPLC using a C8 column. Fractions containing both DNA and Alexa555 signals were pulled together. Estimated labeling efficiency was 90%.

Yeast cells were grown in SCD minimal media supplemented with phosphate at 30°C to an OD600 between 0.2 - 0.8. The hybridization of cells was performed as previously described (Zenklusen et al., 2008).

Images were acquired on Leica DM 5500B epi-fluorescence microscope equipped with Leica DFC 360 FX CCD camera and Leica CTR 5500 light source using 100x oil-immersion objective NA = 1.4. Images were collected in Cy3 (for Alexa555 dye fluorescence), DAPI and differential interference contrast (DIC) channels. Exposure time for the Alexa555 dye was 800 ms. Stacks of images were acquired automatically with 0.25 microns between slices.

ImageJ software was used for image processing and analysis. Stacks of images from separate channels were opened in ImageJ and, typically, 16 slices were chosen for further processing. Background was subtracted from each individual image and a 2-D image was constructed from a 3-D stack using maximum intensity Z-projection procedure. The resulting background was estimated from extracellular space and was constant for the number of slices used. This background was subtracted from the image. Cell nuclei were identified by DAPI staining. In order to count the number of

individual spots per cell, corresponding to individual mRNA molecules, the 2-D Alexa555 image was further treated in the following way: 1.) Process → Filters → Convolve; 2.)Process → Binary → Make binary. The total number of individual signals per cell was determined using the Cell Counter plug-in function.

8. References

Boeger, H., Griesenbeck, J., and Kornberg, R. D. (2008). Nucleosome retention and the stochastic nature of promoter chromatin remodeling for transcription. Cell *133*, 716-726.

Boeger, H., Griesenbeck, J., Strattan, J. S., and Kornberg, R. D. (2003). Nucleosomes unfold completely at a transcriptionally active promoter. Mol Cell *11*, 1587-1598.

Feller, W. (1968). An Introduction to Probability Theory and Its Applications, Vol 1 (New York: John Wiley & Sons, Inc.).

Grimmett, G., and Stirzaker, D. (2001). Probability and Random Processes: Oxford University Press).

Nelder, J. A., and Mead, R. (1965). A simplex method for function minimization. Computer Journal *7*, 308-313.

Raj, A., Peskin, C. S., Tranchina, D., Vargas, D. Y., and Tyagi, S. (2006). Stochastic mRNA Synthesis in Mammalian Cells. PLoS Biol *4*.

Zenklusen, D., Larson, D. R., and Singer, R. H. (2008). Single-RNA counting reveals alternative modes of gene expression in yeast. Nat Struct Mol Biol *15*, 1263-1271.

9. Supplemental Figures

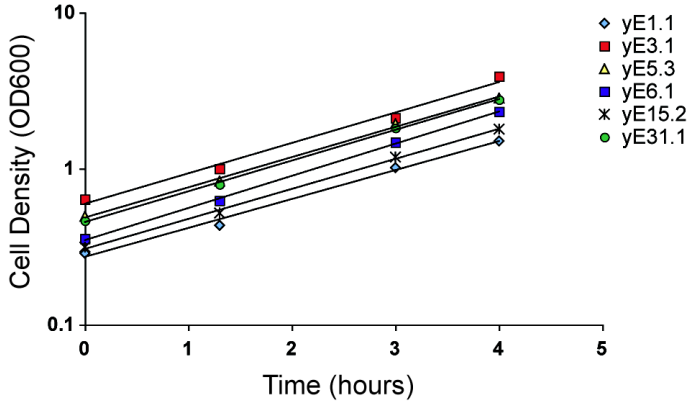

Fig. S1. Growth curves for various *pho4* mutant strains. Mutant strains exhibited similar doubling times within the range of cell densities used for expression and noise measurements.

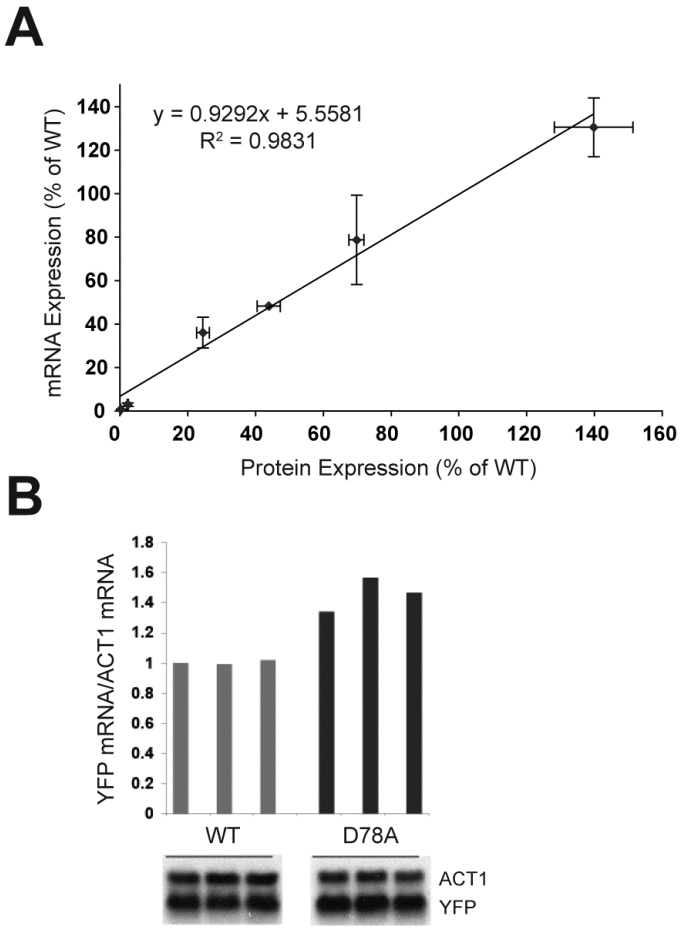

Fig. S2. Average protein and mRNA expression are linearly related. (*A*) Relationship between *PHO5* promoter-controlled YFP-mRNA and YFP expression. Abundance of mRNA was determined by quantitative PCR and expressed as percentage of wild type expression. The *KAP104* transcript was used as an internal

reference. (*B*) Northern blot analysis of *PHO5* promoter-controlled YFP mRNA expression. Total RNA was isolated from three independent cultures each of strains yE1.1 and yE17.4, which express wild type *PHO4* and the D78A mutant, respectively. Total RNA was fractionated by agarose gel electrophoresis, blotted and hybridized with P^{32}-labeled DNA probes spanning the open reading frames of YFP and *ACT1*. Autoradiography images are shown below the histogram, which indicates the amount of YFP-mRNA relative to *ACT1*-mRNA. YFP/*ACT1* signal ratios were normalized to the ratio of one of the three preparations from *PHO4* wild type cells.

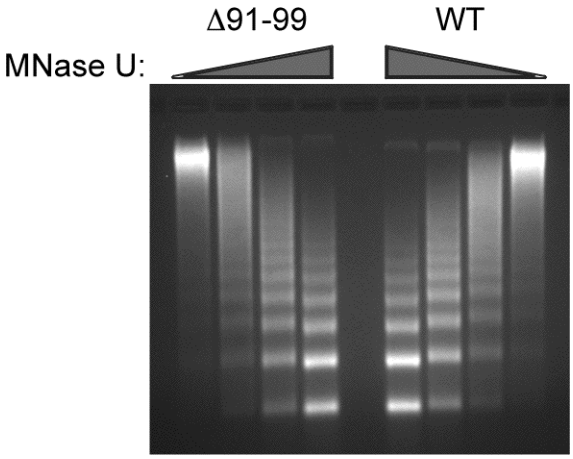

Fig. S3. Micrococcal nuclease digestion of purified nuclei used in ClaI accessibility assays. The same amount of nuclei isolated from wild type *PHO4* (WT) and Δ91-99 cells was digested with 1, 2, 4, and 8 units of nuclease for 20 minutes at 37°C. Isolated DNA was fractionated on a 1.5% agarose gel and stained with ethidium bromide.

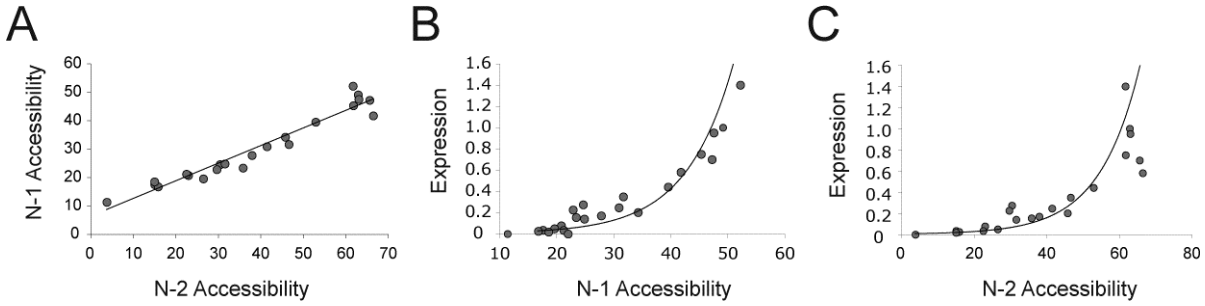

Fig. S4. ClaI accessibility at N-1 and N-2, and *PHO5* expression are exponentially related. (*A*) Relationship between ClaI accessibility at positions N-1 and N-2. (*B*) Relationship between mean expression and ClaI accessibility at N-1. The best-fit line describes an exponential relationship between the two values. A white circle represents the wild type *PHO4* data point. Error bars illustrate standard deviations for expression measurements. (*C*) Relationship between mean expression and ClaI accessibility at N-2. The best-fit line describes an exponential relationship between the two values. Accessibility values measured in *pho4*Δ strain were subtracted from measurements of other strains. White circle represents the wild type *PHO4* data point. Error bars illustrate standard deviations for expression measurements.

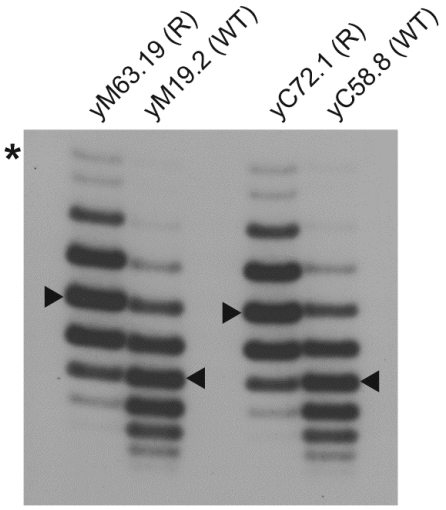

Fig. S5. Differences in the genetic background of strains had no effect on the topoisomer distributions of *PHO5* gene circles. Autoradiography of topoisomer distributions isolated from the indicated strains. Arrowheads indicate centers of topoisomer distributions. Note that distributions isolated from *pho4*Δ strains yM63.19 and yC72.1 were virtually identical. The same was true for *PHO4* strains yM19.2 and yC58.8. An asterisk (*) indicates the position of nicked circle DNA.

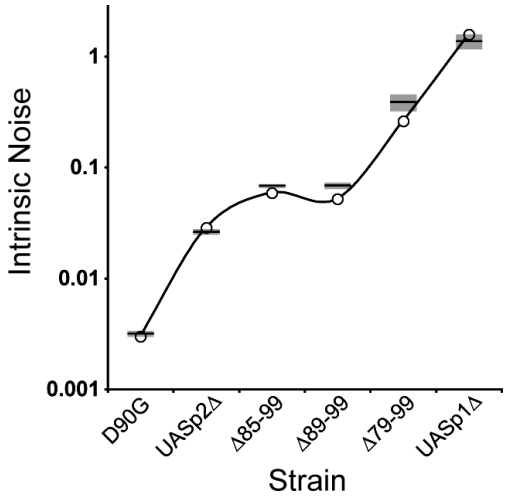

Fig. S6. Predicted and measured noise. Comparison between measured (black horizontal bar ± one standard deviation, gray rectangle) and predicted intrinsic noise of *PHO5* expression (white circle), based on the best-fit solution to regulatory scheme I using the data for 17 rather than 23 strains. The data for the indicated strains were not used for model fitting.

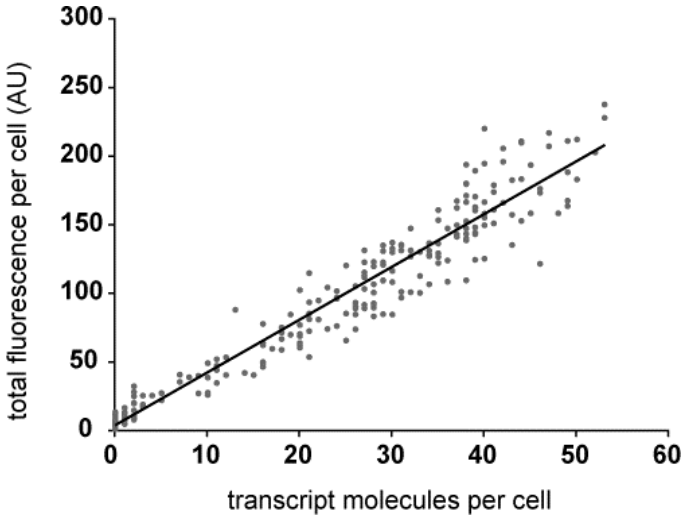

Fig. S7. Relationship of total cell fluorescence and cellular transcript number. In *PHO4 pho80*Δ cells with low mRNA abundance, the number of counted fluorescent dots, corresponding to individual mRNA molecules, were plotted versus the fluorescent signal (in arbitrary units AU) integrated over the entire cell volume. The linear fit allowed for estimation of mRNA molecule numbers in cells where high transcript density prevented the counting of individual molecules.

10. Table SI. Strains and Experimental Measurements

Strain	Gene Circle	YFP Strain	CFP Strain	Diploid Strain	ΔLk°	SD ΔLk°	Expression	SD Expression	Intrinsic Noise	SD Intrinsic
D78A	yM79.8	yE17.4	yE20.11	yE64.1	1.906	0.08	1.4	0.116299	0.00144	0.000128
Wild Type	yM19.2	yE1.1	yE2.1	yE55.1	1.849	0.09	1	0.107134	0.00262	0.000432
D90G	yM85.2	yE16.1	yE19.11	yE63.1	1.806	0.04	0.95	0.075	0.00317	0.000187
D78P	yM84.2	yE15.1	yE18.11	yE62.1	1.735	0.05	0.75	0.062	0.00398	0.000687
Δ[75-78]	yM80.5	yE41.2	yE48.1	yE73.1	1.855	0.15	0.7	0.022645	0.0054	0.0012
Δ[79-86]	yM96.1	yE25.2	yE33.2	yE65.1	1.497	0.01	0.5809	0.060525	0.00864	0.00241
Δ[79-90]	yM68.19	yE6.1	yE11.1	yE58.1	1.363	0.06	0.4414	0.03402	0.01329	0.001748
Δ[78-90]	yM95.1	yE47.3	yE54.1	yE79.1	1.322	0.04	0.35	0.059682	0.01561	0.0014
Δ[91-93]	yM81.3	yE42.3	yE49.1	yE74.1	1.418	0.01	0.2467	0.01881	0.025	0.00351
Δ[76-90]	yM83.5	yE46.2	yE53.1	yE78.1	1.1236	0.05	0.2789	0.080422	0.025421	0.003327
UASp2Δ	yC18.2	yC70.4	yC71.23	yE92.2	1.224	ND	0.25	0.059682	0.02625	0.001511
Δ[75-90]	yM91.1	yE32.2	yE40.5	yE72.1	0.87	0.02	0.226	0.011562	0.037	0.006933
Δ[91-99]	yM82.2	yE31.1	yE39.4	yE71.1	1.386	0.04	0.2021	0.031637	0.0389	0.005073
Δ[87-99]	yM71.19	yE9.2	yE14.2	yE61.1	0.868	0.03	0.17	0.047235	0.061	0.012964
Δ[85-99]	yM89.1	yE29.2	yE37.1	yE69.1	0.915	0.08	0.1406	0.025322	0.068	0.00279
Δ[89-99]	yM90.1	yE30.1	yE38.3	yE70.1	0.981	0.01	0.1545	0.025	0.06843	ND
Δ[82-99]	yM88.1	yE28.1	yE36.1	yE68.1	0.7499	0.02	0.078	0.0139	0.147448	0.028359
Δ[79-92]	yM94.1	yE45.5	yE52.1	yE77.1	0.439	0.02	0.0492	0.00476	0.24876	0.046714
Δ[79-93]	yM86.1	yE26.1	yE34.2	yE66.1	0.45	0.04	0.035	0.016418	0.34436	0.007591
Δ[75-99]	yM67.17	yE5.1	yE10.2	yE57.1	0.298	0.03	0.0255	0.002034	0.37656	0.091428
Δ[79-99]	yM69.15	yE7.3	yE12.8	yE59.1	0.525	0.08	0.0342	0.005025	0.388	0.0677
Δ[79-96]	yM87.1	yE27.1	yE35.2	yE67.1	0.5082	0.003	0.018	0.003291	0.45644	0.004387
UASp1Δ	yC19.3	yC68.7	yC69.5	yE93.6	0.039	0.002	0.01	0.06657	1.367	0.206289
pho4Δ	yM63.19	yE3.1	yE4.1	yE56.1	0	0	0.0043	0.000664	ND	ND

Table SI. Strains and experimental measurements. ΔLk° refers to the linking difference relative to the toposiomer distribution isolated from cells with a transcriptionally repressed *PHO5* promoter (*pho80Δ pho4Δ*

strain). Δ equally refers to the absence of the Pho4 protein and deletion of the *PHO4* gene. ND, not determined; SD, standard deviation. All indicated strains are *pho80Δ*.

11. Table SII. Kinetic parameters for activator and UASp mutants.

Kinetic Parameters (Generated from 21 Strains)								
Mutant	**z_1**	**z_2**	**z_3**	**z_4**	**z_5**	**z_6**	**z_7**	**z_8**
D78A	21.2	78.8	118.4	49.7	818.8	63.3	405.5	443.0
WT	21.2	78.8	118.4	126.9	230.2	63.3	405.5	443.0
D90G	21.2	78.8	118.4	101.2	208.7	63.3	405.5	443.0
D78P	21.2	78.8	118.4	96.4	123.1	63.3	405.5	443.0
75-78	21.2	78.8	118.4	234.0	92.9	63.3	405.5	443.0
79-86	21.2	78.8	118.4	45.5	94.3	63.3	405.5	443.0
79-90	21.2	78.8	118.4	36.1	66.7	63.3	405.5	443.0
78-90	21.2	78.8	118.4	36.3	48.9	63.3	405.5	443.0
91-93	21.2	78.8	118.4	56.3	27.7	63.3	405.5	443.0
76-90	21.2	78.8	118.4	22.5	43.3	63.3	405.5	443.0
UASp2	21.2	78.8	118.4	31.3	33.7	63.3	405.5	443.0
75-90	21.2	78.8	118.4	12.0	44.1	63.3	405.5	443.0
91-99	21.2	78.8	118.4	53.8	22.3	63.3	405.5	443.0
87-99	21.2	78.8	118.4	13.0	30.6	63.3	405.5	443.0
85-99	21.2	78.8	118.4	15.4	22.8	63.3	405.5	443.0
89-99	21.2	78.8	118.4	18.1	23.7	63.3	405.5	443.0
82-99	21.2	78.8	118.4	10.7	14.4	63.3	405.5	443.0
79-92	21.2	78.8	118.4	4.3	15.4	63.3	405.5	443.0
79-93	21.2	78.8	118.4	4.6	8.5	63.3	405.5	443.0
75-99	21.2	78.8	118.4	2.6	11.4	63.3	405.5	443.0
79-99	21.2	78.8	118.4	5.9	6.0	63.3	405.5	443.0
79-96	21.2	78.8	118.4	5.8	4.6	63.3	405.5	443.0
UASp1	21.2	78.8	118.4	0.2	38.5	63.3	405.5	443.0

Validation of Kinetic Parameters (Generated from 17 Strains)								
Mutant	**z_1**	**z_2**	**z_3**	**z_4**	**z_5**	**z_6**	**z_7**	**z_8**
D90G	16.6	51.0	86.9	69.4	233.0	72.2	401.1	137.9
85-99	16.6	51.0	86.9	11.3	25.7	72.2	401.1	137.9
89-99	16.6	51.0	86.9	13.2	26.8	72.2	401.1	137.9
UASp2	16.6	51.0	86.9	22.2	38.0	72.2	401.1	137.9

79-99	16.6	51.0	86.9	4.5	9.7	72.2	401.1	137.9
UASp1	16.6	51.0	86.9	0.2	43.6	72.2	401.1	137.9

Table SII. Kinetic parameters for activator and UAS mutants. Values for the kinetic parameters (transition probabilities per hour per molecule) of the expression process were derived by minimizing the noise error function (see equation [28], section 1.) for regulatory scheme I using either 21 activator (mutant) strains (upper panel), or 17 activator strains (lower panel). In the latter case, parameters are indicated only for strains whose data were not used for fitting (see Fig. S6).

12. Table SIII - Strains and Plasmids

Strain	Parental Strain	Plasmids	Genotype
YS18			MATα his3-11 his3-15 leu2-3 leu2-112 canR ura3Δ5
yM1.12	YS18	pM51.1	MATα his3-11 his3-15 leu2-3 leu2-112 canR ura3Δ5 pho5Δ:URA3
yM17.3	yM1.12	pM67.6	MATα his3-11 his3-15 leu2-3 leu2-112 canR ura3Δ5 pho5Δ:URA3 pho80Δ::HIS3
yM19.2	yM17.3	pM70.1	MATα his3-11 his3-15 leu2-3 leu2-112 canR ura3Δ5 pho5[GC, <TATA>] pho80Δ::HIS3
yM63.19	yM19.2	pCM4.5	MATα his3-11 his3-15 leu2-3 leu2-112 canR ura3Δ5 pho5[GC, <TATA>] pho80Δ::HIS3 pho4Δ::URA3
yM67.17	yM63.19	pCM5.2	MATα his3-11 his3-15 leu2-3 leu2-112 canR ura3Δ5 pho5[GC, <TATA>] pho80Δ::HIS3 pho4-Δ75-99
yM68.19	yM63.19	pCM6.3	MATα his3-11 his3-15 leu2-3 leu2-112 canR ura3Δ5 pho5[GC, <TATA>] pho80Δ::HIS3 pho4-Δ79-90
yM69.14	yM63.19	pCM7.3	MATα his3-11 his3-15 leu2-3 leu2-112 canR ura3Δ5 pho5[GC, <TATA>] pho80Δ::HIS3 pho4-Δ79-99
yM71.19	yM63.19	pCM10.3	MATα his3-11 his3-15 leu2-3 leu2-112 canR ura3Δ5 pho5[GC, <TATA>] pho80Δ::HIS3 pho4-Δ87-99
yM79.8	yM63.19	pCM39.1	MATα his3-11 his3-15 leu2-3 leu2-112 canR ura3Δ5 pho5[GC, <TATA>] pho80Δ::HIS3 pho4-D78A
yM80.5	yM63.19	pCM67.1	MATα his3-11 his3-15 leu2-3 leu2-112 canR ura3Δ5 pho5[GC, <TATA>] pho80Δ::HIS3 pho4-Δ75-78
yM81.3	yM63.19	pCM68.1	MATα his3-11 his3-15 leu2-3 leu2-112 canR ura3Δ5 pho5[GC, <TATA>] pho80Δ::HIS3 pho4-Δ91-93
yM82.2	yM63.19	pCM63.2	MATα his3-11 his3-15 leu2-3 leu2-112 canR ura3Δ5 pho5[GC, <TATA>] pho80Δ::HIS3 pho4-Δ91-99
yM83.5	yM63.19	pCM72.1	MATα his3-11 his3-15 leu2-3 leu2-112 canR ura3Δ5 pho5[GC, <TATA>] pho80Δ::HIS3 pho4-Δ76-90
yM84.2	yM63.19	pCM37.1	MATα his3-11 his3-15 leu2-3 leu2-112 canR ura3Δ5 pho5[GC, <TATA>] pho80Δ::HIS3 pho4-D78P
yM85.2	yM63.19	pCM38.1	MATα his3-11 his3-15 leu2-3 leu2-112 canR ura3Δ5 pho5[GC, <TATA>] pho80Δ::HIS3 pho4-D90G
yM86.1	yM63.19	pCM58.2	MATα his3-11 his3-15 leu2-3 leu2-112 canR ura3Δ5 pho5[GC, <TATA>] pho80Δ::HIS3 pho4-Δ79-93
yM87.1	yM63.19	pCM59.1	MATα his3-11 his3-15 leu2-3 leu2-112 canR ura3Δ5 pho5[GC, <TATA>] pho80Δ::HIS3 pho4-Δ79-96
yM88.1	yM63.19	pCM60.1	MATα his3-11 his3-15 leu2-3 leu2-112 canR ura3Δ5 pho5[GC, <TATA>] pho80Δ::HIS3 pho4-Δ82-99
yM89.1	yM63.19	pCM61.5	MATα his3-11 his3-15 leu2-3 leu2-112 canR ura3Δ5 pho5[GC, <TATA>] pho80Δ::HIS3 pho4-Δ85-99
yM90.1	yM63.19	pCM62.1	MATα his3-11 his3-15 leu2-3 leu2-112 canR ura3Δ5 pho5[GC, <TATA>] pho80Δ::HIS3 pho4-Δ89-99
yM91.1	yM63.19	pCM64.2	MATα his3-11 his3-15 leu2-3 leu2-112 canR ura3Δ5 pho5[GC, <TATA>] pho80Δ::HIS3 pho4-Δ75-90
yM94.1	yM63.19	pCM71.1	MATα his3-11 his3-15 leu2-3 leu2-112 canR ura3Δ5 pho5[GC, <TATA>] pho80Δ::HIS3 pho4-Δ79-92
yM95.1	yM63.19	pCM73.2	MATα his3-11 his3-15 leu2-3 leu2-112 canR ura3Δ5 pho5[GC, <TATA>] pho80Δ::HIS3 pho4-Δ78-90
yM96.1	yM63.19	pCM57.1	MATα his3-11 his3-15 leu2-3 leu2-112 canR ura3Δ5 pho5[GC, <TATA>] pho80Δ::HIS3 pho4-Δ79-86
yC18.2	yM17.3	pCM54.1	MATa his3-11 his3-15 leu2-3 leu2-112 canR ura3Δ5 pho5[GC, <TATA>]:UASP2mut pho80Δ::HIS3
yC19.3	yM17.3	pCM55.1	MATa his3-11 his3-15 leu2-3 leu2-112 canR ura3Δ5 pho5[GC, <TATA>]:UASP1mut pho80Δ::HIS3
EY1655	O'Shea Lab		MATα leu2-3,112 trp1-1 can1-100 ura3-1 his3-11,15 GAL+ pho5Δ::YFP-HIS3
EY2343	O'Shea Lab		MATa leu2-3,112 trp1-1 can1-100 ura3-1 ade2-1 his3-11,15 GAL+ pho5Δ::CFP-KanR
yE1.1	EY1655	pCM43.12	MATα leu2-3,112 trp1-1 can1-100 ura3-1 his3-11,15 GAL+ pho5Δ::YFP-HIS3 pho80Δ::LEU2
yE2.1	EY2343	pCM43.12	MATa leu2-3,112 trp1-1 can1-100 ura3-1 ade2-1 his3-11,15 GAL+ pho5Δ::CFP-KanR pho80Δ::LEU2
yE3.1	yE1.1	pCM4.5	MATα leu2-3,112 trp1-1 can1-100 ura3-1 his3-11,15 GAL+ pho5Δ::YFP-HIS3 pho80Δ::LEU2 pho4Δ::URA3
yE4.1	yE2.1	pCM4.5	MATa leu2-3,112 trp1-1 can1-100 ura3-1 ade2-1 his3-11,15 GAL+ pho5Δ::CFP-KanR pho80Δ::LEU2 pho4Δ::URA3
yE5.1	yE3.1	pCM5.2	MATα leu2-3,112 trp1-1 can1-100 ura3-1 his3-11,15 GAL+ pho5Δ::YFP-HIS3 pho80Δ::LEU2 pho4-Δ75-99
yE6.1	yE3.1	pCM6.3	MATα leu2-3,112 trp1-1 can1-100 ura3-1 his3-11,15 GAL+ pho5Δ::YFP-HIS3 pho80Δ::LEU2 pho4-Δ79-90
yE7.3	yE3.1	pCM7.3	MATα leu2-3,112 trp1-1 can1-100 ura3-1 his3-11,15 GAL+ pho5Δ::YFP-HIS3 pho80Δ::LEU2 pho4-Δ79-99
yE9.2	yE3.1	pCM10.3	MATα leu2-3,112 trp1-1 can1-100 ura3-1 his3-11,15 GAL+ pho5Δ::YFP-HIS3 pho80Δ::LEU2 pho4-Δ87-99
yE10.2	yE4.1	pCM5.2	MATa leu2-3,112 trp1-1 can1-100 ura3-1 ade2-1 his3-11,15 GAL+ pho5Δ::CFP-KanR pho80Δ::LEU2 pho4-Δ75-99
yE11.1	yE4.1	pCM6.3	MATa leu2-3,112 trp1-1 can1-100 ura3-1 ade2-1 his3-11,15 GAL+ pho5Δ::CFP-KanR pho80Δ::LEU2 pho4-Δ79-90
yE12.8	yE4.1	pCM7.3	MATa leu2-3,112 trp1-1 can1-100 ura3-1 ade2-1 his3-11,15 GAL+ pho5Δ::CFP-KanR pho80Δ::LEU2 pho4-Δ79-99
yE14.2	yE4.1	pCM10.3	MATa leu2-3,112 trp1-1 can1-100 ura3-1 ade2-1 his3-11,15 GAL+ pho5Δ::CFP-KanR pho80Δ::LEU2 pho4-Δ87-99
yE15.1	yE3.1	pCM37.1	MATα leu2-3,112 trp1-1 can1-100 ura3-1 his3-11,15 GAL+ pho5Δ::YFP-HIS3 pho80Δ::LEU2 pho4-D78P
yE16.1	yE3.1	pCM38.1	MATα leu2-3,112 trp1-1 can1-100 ura3-1 his3-11,15 GAL+ pho5Δ::YFP-HIS3 pho80Δ::LEU2 pho4-D90G
yE17.4	yE3.1	pCM39.1	MATα leu2-3,112 trp1-1 can1-100 ura3-1 his3-11,15 GAL+ pho5Δ::YFP-HIS3 pho80Δ::LEU2 pho4-D78A
yE18.11	yE4.1	pCM37.1	MATa leu2-3,112 trp1-1 can1-100 ura3-1 ade2-1 his3-11,15 GAL+ pho5Δ::CFP-KanR pho80Δ::LEU2 pho4-D78P

yE19.11	yE4.1	pCM38.1	MATa leu2-3,112 trp1-1 can1-100 ura3-1 ade2-1 his3-11,15 GAL+ pho5Δ::CFP-KanR pho80Δ::LEU2 pho4-D90G
yE20.11	yE4.1	pCM39.1	MATa leu2-3,112 trp1-1 can1-100 ura3-1 ade2-1 his3-11,15 GAL+ pho5Δ::CFP-KanR pho80Δ::LEU2 pho4-D78A
yE21.3	yE1.1	pM51.1	MATα leu2-3,112 trp1-1 can1-100 ura3-1 his3-11,15 GAL+ pho5Δ::URA3 pho80Δ::LEU2
yE22.1	yE2.1	pM51.1	MATa leu2-3,112 trp1-1 can1-100 ura3-1 ade2-1 his3-11,15 GAL+ pho5Δ::URA3 pho80Δ::LEU2
yE25.2	yE3.1	pCM57.1	MATα leu2-3,112 trp1-1 can1-100 ura3-1 his3-11,15 GAL+ pho5Δ::YFP-HIS3 pho80Δ::LEU2 pho4-Δ79-86
yE26.1	yE3.1	pCM58.2	MATα leu2-3,112 trp1-1 can1-100 ura3-1 his3-11,15 GAL+ pho5Δ::YFP-HIS3 pho80Δ::LEU2 pho4-Δ79-93
yE27.1	yE3.1	pCM59.1	MATα leu2-3,112 trp1-1 can1-100 ura3-1 his3-11,15 GAL+ pho5Δ::YFP-HIS3 pho80Δ::LEU2 pho4-Δ79-96
yE28.1	yE3.1	pCM60.1	MATα leu2-3,112 trp1-1 can1-100 ura3-1 his3-11,15 GAL+ pho5Δ::YFP-HIS3 pho80Δ::LEU2 pho4-Δ82-99
yE29.2	yE3.1	pCM61.5	MATα leu2-3,112 trp1-1 can1-100 ura3-1 his3-11,15 GAL+ pho5Δ::YFP-HIS3 pho80Δ::LEU2 pho4-Δ85-99
yE30.1	yE3.1	pCM62.1	MATα leu2-3,112 trp1-1 can1-100 ura3-1 his3-11,15 GAL+ pho5Δ::YFP-HIS3 pho80Δ::LEU2 pho4-Δ89-99
yE31.1	yE3.1	pCM63.1	MATα leu2-3,112 trp1-1 can1-100 ura3-1 his3-11,15 GAL+ pho5Δ::YFP-HIS3 pho80Δ::LEU2 pho4-Δ91-99
yE32.2	yE3.1	pCM64.1	MATα leu2-3,112 trp1-1 can1-100 ura3-1 his3-11,15 GAL+ pho5Δ::YFP-HIS3 pho80Δ::LEU2 pho4-Δ75-90
yE33.2	yE4.1	pCM57.1	MATa leu2-3,112 trp1-1 can1-100 ura3-1 ade2-1 his3-11,15 GAL+ pho5Δ::CFP-KanR pho80Δ::LEU2 pho4-Δ79-86
yE34.2	yE4.1	pCM58.2	MATa leu2-3,112 trp1-1 can1-100 ura3-1 ade2-1 his3-11,15 GAL+ pho5Δ::CFP-KanR pho80Δ::LEU2 pho4-Δ79-93
yE35.2	yE4.1	pCM59.1	MATa leu2-3,112 trp1-1 can1-100 ura3-1 ade2-1 his3-11,15 GAL+ pho5Δ::CFP-KanR pho80Δ::LEU2 pho4-Δ79-96
yE36.1	yE4.1	pCM60.1	MATa leu2-3,112 trp1-1 can1-100 ura3-1 ade2-1 his3-11,15 GAL+ pho5Δ::CFP-KanR pho80Δ::LEU2 pho4-Δ82-99
yE37.1	yE4.1	pCM61.5	MATa leu2-3,112 trp1-1 can1-100 ura3-1 ade2-1 his3-11,15 GAL+ pho5Δ::CFP-KanR pho80Δ::LEU2 pho4-Δ85-99
yE38.3	yE4.1	pCM62.1	MATa leu2-3,112 trp1-1 can1-100 ura3-1 ade2-1 his3-11,15 GAL+ pho5Δ::CFP-KanR pho80Δ::LEU2 pho4-Δ89-99
yE39.4	yE4.1	pCM63.1	MATa leu2-3,112 trp1-1 can1-100 ura3-1 ade2-1 his3-11,15 GAL+ pho5Δ::CFP-KanR pho80Δ::LEU2 pho4-Δ91-99
yE40.5	yE4.1	pCM64.1	MATa leu2-3,112 trp1-1 can1-100 ura3-1 ade2-1 his3-11,15 GAL+ pho5Δ::CFP-KanR pho80Δ::LEU2 pho4-Δ75-90
yE41.2	yE3.1	pCM67.1	MATα leu2-3,112 trp1-1 can1-100 ura3-1 his3-11,15 GAL+ pho5Δ::YFP-HIS3 pho80Δ::LEU2 pho4-Δ75-78
yE42.3	yE3.1	pCM68.1	MATα leu2-3,112 trp1-1 can1-100 ura3-1 his3-11,15 GAL+ pho5Δ::YFP-HIS3 pho80Δ::LEU2 pho4-Δ91-93
yE45.5	yE3.1	pCM71.1	MATα leu2-3,112 trp1-1 can1-100 ura3-1 his3-11,15 GAL+ pho5Δ::YFP-HIS3 pho80Δ::LEU2 pho4-Δ79-92
yE46.2	yE3.1	pCM72.1	MATα leu2-3,112 trp1-1 can1-100 ura3-1 his3-11,15 GAL+ pho5Δ::YFP-HIS3 pho80Δ::LEU2 pho4-Δ76-90
yE47.3	yE3.1	pCM73.2	MATα leu2-3,112 trp1-1 can1-100 ura3-1 his3-11,15 GAL+ pho5Δ::YFP-HIS3 pho80Δ::LEU2 pho4-Δ78-90
yE48.1	yE4.1	pCM67.1	MATa leu2-3,112 trp1-1 can1-100 ura3-1 ade2-1 his3-11,15 GAL+ pho5Δ::CFP-KanR pho80Δ::LEU2 pho4-Δ75-78
yE49.1	yE4.1	pCM68.1	MATa leu2-3,112 trp1-1 can1-100 ura3-1 ade2-1 his3-11,15 GAL+ pho5Δ::CFP-KanR pho80Δ::LEU2 pho4-Δ91-93
yE52.1	yE4.1	pCM71.1	MATa leu2-3,112 trp1-1 can1-100 ura3-1 ade2-1 his3-11,15 GAL+ pho5Δ::CFP-KanR pho80Δ::LEU2 pho4-Δ79-92
yE53.1	yE4.1	pCM72.1	MATa leu2-3,112 trp1-1 can1-100 ura3-1 ade2-1 his3-11,15 GAL+ pho5Δ::CFP-KanR pho80Δ::LEU2 pho4-Δ76-90
yE54.1	yE4.1	pCM73.2	MATa leu2-3,112 trp1-1 can1-100 ura3-1 ade2-1 his3-11,15 GAL+ pho5Δ::CFP-KanR pho80Δ::LEU2 pho4-Δ78-90
yC56.11	yE21.3	pM67.6	MATα leu2-3,112 trp1-1 can1-100 ura3-1 his3-11,15 GAL+ pho5Δ::URA3 pho80Δ::HIS3
yC58.8	yC56.11	pM70.1	MATα leu2-3,112 trp1-1 can1-100 ura3-1 his3-11,15 GAL+ pho5[GC, <TATA>] pho80Δ::HIS3
yC66.2	yE21.3	pCM97.2	MATα leu2-3,112 trp1-1 can1-100 ura3-1 his3-11,15 GAL+ PHO5-YFP pho80Δ::LEU2
yC67.1	yE22.1	pCM98.1	MATa leu2-3,112 trp1-1 can1-100 ura3-1 ade2-1 his3-11,15 GAL+ PHO5-CFP pho80Δ::LEU2
yC68.7	yE21.3	pCM99.1	MATα leu2-3,112 trp1-1 can1-100 ura3-1 his3-11,15 GAL+ PHO5[UASP1mut]-YFP pho80Δ::LEU2
yC69.5	yE22.1	pCM100.1	MATa leu2-3,112 trp1-1 can1-100 ura3-1 ade2-1 his3-11,15 GAL+ PHO5[UASP1mut]-CFP pho80Δ::LEU2
yC70.4	yE21.3	pCM101.1	MATα leu2-3,112 trp1-1 can1-100 ura3-1 his3-11,15 GAL+ PHO5[UASP2mut]-YFP pho80Δ::LEU2
yC71.23	yE22.1	pCM102.1	MATa leu2-3,112 trp1-1 can1-100 ura3-1 ade2-1 his3-11,15 GAL+ PHO5[UASP2mut]-CFP pho80Δ::LEU2
yC72.1	yC58.8	pCM90.1	MATα leu2-3,112 trp1-1 can1-100 ura3-1 his3-11,15 GAL+ pho5[GC, <TATA>] pho80Δ::HIS3 pho4Δ::URA3

Diploid Strain	Parental Strains	Genotype
yE55.1	yE1.1 x yE2.1	MATα /MATa leu2-3,112/leu2-3,112 trp1-1/trp1-1 can1-100/can1-100 ura3-1/ura3-1 ADE2/ade2-1 his3-11,15/his3-11,15 GAL+/GAL+ pho5Δ::YFP-HIS3/pho5Δ::CFP-KanR pho80Δ::LEU2/pho80Δ::LEU2
yE56.1	yE3.1 x yE4.1	MATα /MATa leu2-3,112/leu2-3,112 trp1-1/trp1-1 can1-100/can1-100 ura3-1/ura3-1 ADE2/ade2-1 his3-11,15/his3-11,15 GAL+/GAL+ pho5Δ::YFP-HIS3/pho5Δ::CFP-KanR pho80Δ::LEU2/pho80Δ::LEU2 pho4Δ::URA3/pho4Δ::URA3
yE57.1	yE5.1 x yE10.2	MATα /MATa leu2-3,112/leu2-3,112 trp1-1/trp1-1 can1-100/can1-100 ura3-1/ura3-1 ADE2/ade2-1 his3-11,15/his3-11,15 GAL+/GAL+ pho5Δ::YFP-HIS3/pho5Δ::CFP-KanR pho80Δ::LEU2/pho80Δ::LEU2 pho4-Δ75-99/pho4-Δ75-99
yE58.1	yE6.1 x yE11.1	MATα /MATa leu2-3,112/leu2-3,112 trp1-1/trp1-1 can1-100/can1-100 ura3-1/ura3-1 ADE2/ade2-1 his3-11,15/his3-11,15 GAL+/GAL+ pho5Δ::YFP-HIS3/pho5Δ::CFP-KanR pho80Δ::LEU2/pho80Δ::LEU2 pho4-Δ79-90/pho4-Δ79-90
yE59.1	yE7.3 x yE12.8	MATα /MATa leu2-3,112/leu2-3,112 trp1-1/trp1-1 can1-100/can1-100 ura3-1/ura3-1 ADE2/ade2-1 his3-11,15/his3-11,15 GAL+/GAL+ pho5Δ::YFP-HIS3/pho5Δ::CFP-KanR pho80Δ::LEU2/pho80Δ::LEU2 pho4-Δ79-99/pho4-Δ79-99
yE61.1	yE9.2 x yE14.2	MATα /MATa leu2-3,112/leu2-3,112 trp1-1/trp1-1 can1-100/can1-100 ura3-1/ura3-1 ADE2/ade2-1 his3-11,15/his3-11,15 GAL+/GAL+ pho5Δ::YFP-HIS3/pho5Δ::CFP-KanR pho80Δ::LEU2/pho80Δ::LEU2 pho4-Δ87-99/pho4-Δ87-99
yE62.1	yE15.1 x yE18.11	MATα /MATa leu2-3,112/leu2-3,112 trp1-1/trp1-1 can1-100/can1-100 ura3-1/ura3-1 ADE2/ade2-1 his3-11,15/his3-11,15 GAL+/GAL+ pho5Δ::YFP-HIS3/pho5Δ::CFP-KanR pho80Δ::LEU2/pho80Δ::LEU2 pho4-D78P/pho4-D78P
yE63.1	yE16.1 x yE19.11	MATα /MATa leu2-3,112/leu2-3,112 trp1-1/trp1-1 can1-100/can1-100 ura3-1/ura3-1 ADE2/ade2-1 his3-11,15/his3-11,15 GAL+/GAL+ pho5Δ::YFP-HIS3/pho5Δ::CFP-KanR pho80Δ::LEU2/pho80Δ::LEU2 pho4-D90G/pho4-D90G
yE64.1	yE17.4 x yE20.11	MATα /MATa leu2-3,112/leu2-3,112 trp1-1/trp1-1 can1-100/can1-100 ura3-1/ura3-1 ADE2/ade2-1 his3-11,15/his3-11,15 GAL+/GAL+ pho5Δ::YFP-HIS3/pho5Δ::CFP-KanR pho80Δ::LEU2/pho80Δ::LEU2 pho4-D78A/pho4-D78A
yE65.1	yE25.2 x yE33.2	MATα /MATa leu2-3,112/leu2-3,112 trp1-1/trp1-1 can1-100/can1-100 ura3-1/ura3-1 ADE2/ade2-1 his3-11,15/his3-11,15 GAL+/GAL+ pho5Δ::YFP-HIS3/pho5Δ::CFP-KanR pho80Δ::LEU2/pho80Δ::LEU2 pho4-Δ79-86/pho4-Δ79-86

yE66.1	yE26.1 x yE34.2	MATα /MATa leu2-3,112/leu2-3,112 trp1-1/trp1-1 can1-100/can1-100 ura3-1/ura3-1 ADE2/ade2-1 his3-11,15/his3-11,15 GAL+/GAL+ pho5Δ::YFP-HIS3/pho5Δ::CFP-KanR pho80Δ::LEU2/pho80Δ::LEU2 pho4-Δ79-93/pho4-Δ79-93
yE67.1	yE27.1 x yE35.2	MATα /MATa leu2-3,112/leu2-3,112 trp1-1/trp1-1 can1-100/can1-100 ura3-1/ura3-1 ADE2/ade2-1 his3-11,15/his3-11,15 GAL+/GAL+ pho5Δ::YFP-HIS3/pho5Δ::CFP-KanR pho80Δ::LEU2/pho80Δ::LEU2 pho4-Δ79-96/pho4-Δ79-96
yE68.1	yE28.1 x yE36.1	MATα /MATa leu2-3,112/leu2-3,112 trp1-1/trp1-1 can1-100/can1-100 ura3-1/ura3-1 ADE2/ade2-1 his3-11,15/his3-11,15 GAL+/GAL+ pho5Δ::YFP-HIS3/pho5Δ::CFP-KanR pho80Δ::LEU2/pho80Δ::LEU2 pho4-Δ82-99/pho4-Δ82-99
yE69.1	yE29.2 x yE37.1	MATα /MATa leu2-3,112/leu2-3,112 trp1-1/trp1-1 can1-100/can1-100 ura3-1/ura3-1 ADE2/ade2-1 his3-11,15/his3-11,15 GAL+/GAL+ pho5Δ::YFP-HIS3/pho5Δ::CFP-KanR pho80Δ::LEU2/pho80Δ::LEU2 pho4-Δ85-99/pho4-Δ85-99
yE70.1	yE30.1 x yE38.3	MATα /MATa leu2-3,112/leu2-3,112 trp1-1/trp1-1 can1-100/can1-100 ura3-1/ura3-1 ADE2/ade2-1 his3-11,15/his3-11,15 GAL+/GAL+ pho5Δ::YFP-HIS3/pho5Δ::CFP-KanR pho80Δ::LEU2/pho80Δ::LEU2 pho4-Δ89-99/pho4-Δ89-99
yE71.1	yE31.1 x yE39.4	MATα /MATa leu2-3,112/leu2-3,112 trp1-1/trp1-1 can1-100/can1-100 ura3-1/ura3-1 ADE2/ade2-1 his3-11,15/his3-11,15 GAL+/GAL+ pho5Δ::YFP-HIS3/pho5Δ::CFP-KanR pho80Δ::LEU2/pho80Δ::LEU2 pho4-Δ91-99/pho4-Δ91-99
yE72.1	yE32.1 x yE40.5	MATα /MATa leu2-3,112/leu2-3,112 trp1-1/trp1-1 can1-100/can1-100 ura3-1/ura3-1 ADE2/ade2-1 his3-11,15/his3-11,15 GAL+/GAL+ pho5Δ::YFP-HIS3/pho5Δ::CFP-KanR pho80Δ::LEU2/pho80Δ::LEU2 pho4-Δ75-90/pho4-Δ75-90
yE73.1	yE41.1 x yE48.1	MATa/MATa leu2-3,112/leu2-3,112 trp1-1/trp1-1 can1-100/can1-100 ura3-1/ura3-1 ADE2/ade2-1 his3-11,15/his3-11,15 GAL+/GAL+ pho5Δ::YFP-HIS3/pho5Δ::CFP-KanR pho80Δ::LEU2/pho80Δ::LEU2 pho4-Δ75-78/pho4-Δ75-78
yE74.1	yE42.1 x yE49.1	MATa/MATa leu2-3,112/leu2-3,112 trp1-1/trp1-1 can1-100/can1-100 ura3-1/ura3-1 ADE2/ade2-1 his3-11,15/his3-11,15 GAL+/GAL+ pho5Δ::YFP-HIS3/pho5Δ::CFP-KanR pho80Δ::LEU2/pho80Δ::LEU2 pho4-Δ91-93/pho4-Δ91-93
yE77.1	yE45.2 x yE52.1	MATa/MATa leu2-3,112/leu2-3,112 trp1-1/trp1-1 can1-100/can1-100 ura3-1/ura3-1 ADE2/ade2-1 his3-11,15/his3-11,15 GAL+/GAL+ pho5Δ::YFP-HIS3/pho5Δ::CFP-KanR pho80Δ::LEU2/pho80Δ::LEU2 pho4-Δ79-92/pho4-Δ79-92
yE78.1	yE46.1 x yE53.1	MATa/MATa leu2-3,112/leu2-3,112 trp1-1/trp1-1 can1-100/can1-100 ura3-1/ura3-1 ADE2/ade2-1 his3-11,15/his3-11,15 GAL+/GAL+ pho5Δ::YFP-HIS3/pho5Δ::CFP-KanR pho80Δ::LEU2/pho80Δ::LEU2 pho4-Δ76-90/pho4-Δ76-90
yE79.1	yE47.1 x yE54.1	MATa/MATa leu2-3,112/leu2-3,112 trp1-1/trp1-1 can1-100/can1-100 ura3-1/ura3-1 ADE2/ade2-1 his3-11,15/his3-11,15 GAL+/GAL+ pho5Δ::YFP-HIS3/pho5Δ::CFP-KanR pho80Δ::LEU2/pho80Δ::LEU2 pho4-Δ78-90/pho4-Δ78-90
yE92.2	yC70.4 x yC71.23	MATa/MATa leu2-3,112/leu2-3,112 trp1-1/trp1-1 can1-100/can1-100 ura3-1/ura3-1 ADE2/ade2-1 his3-11,15/his3-11,15 GAL+/GAL+ PHO5[UASP2mut]-YFP/PHO5[UASP2mut]-CFP pho80Δ::LEU2/pho80Δ::LEU2
yE93.6	yC68.7 x yC69.5	MATa/MATa leu2-3,112/leu2-3,112 trp1-1/trp1-1 can1-100/can1-100 ura3-1/ura3-1 ADE2/ade2-1 his3-11,15/his3-11,15 GAL+/GAL+ PHO5[UASP1mut]-YFP/PHO5[UASP1mut]-CFP pho80Δ::LEU2/pho80Δ::LEU2

Table SIII. Strains and Plasmids. Strains constructed for this study are listed above, including the identification of parental strains and the plasmids used to create them. Strain yM1.12, yM17.3, and yM19.2 had been described earlier (Boeger et al., 2003).